PHYSICAL REVIEW B, VOLUME 65, 140504(R)

Interlayer tunneling spectroscopy of $Bi_2Sr_2CaCu_2O_{8+\delta}$: A look from inside on the doping phase diagram of high-T_c superconductors

V. M. Krasnov
Department of Microelectronics and Nanoscience, Chalmers University of Technology, S-41296 Göteborg, Sweden
(Received 2 January 2002; published 22 March 2002)

A systematic, doping-dependent interlayer tunneling spectroscopy of Bi2212 high-T_c superconductor is presented. An improved resolution made it possible to simultaneously trace the superconducting gap (SG) and the normal state pseudogap (PG) in a close vicinity of T_c and to analyze closing of the PG at T^*. The obtained doping phase diagram exhibits a critical doping point for appearance of the PG and a characteristic crossing of the SG and the PG close to the optimal doping. This points towards coexistence of two different and competing order parameters in Bi2212. Experimental data indicate that the SG can form a combined (large) gap with the PG at $T<T_c$ and that the interlayer tunneling becomes progressively incoherent with decreasing doping.

DOI: 10.1103/PhysRevB.65.140504 PACS number(s): 74.50.+r, 74.25.−q, 74.72.Hs, 74.80.Dm

Observation of an energy gap in the electronic density of states (DOS) had a decisive role in understanding of low-T_c superconductivity.[1] However, fifteen years after discovery of high-T_c superconductors (HTSC), there is still no consensus about HTSC energy gap. Several experiments revealed different energy scales in HTSC.[2–7] One of those, a normal state pseudogap (PG), persists at $T>T_c$.[2–8] The origin of the PG is an intriguing open question, which is crucial for understanding HTSC. Currently, the scientific community is divided, believing either in superconducting or nonsuperconducting origins of the PG. The resolution can be provided by a doping phase diagram, both because oxygen doping is the most critical HTSC parameter (HTSC can be altered from a metal to an antiferromagnetic insulator by decreasing *O* content) and because distinctly different diagrams are expected for different scenarios.[6] In a superconducting scenario, the PG represents the pairing energy, which can be finite at $T>T_c$ in a strong-coupling case. The smaller gap represents the energy required for maintenance of a long-range coherence[2] at $T<T_c$. Those two energies should *merge* in the overdoped (OD) region, as the weak-coupling limit is approached. If, on the contrary, the PG appears abruptly at some critical doping point p_c and the PG *crosses* the superconducting gap (SG) at the phase diagram, it would correspond to a nonsuperconducting PG,[6] which develops in the underdoped (UD) region at the expense of the SG.

The present state of confusion requires further studies using advanced experimental techniques. One of those is an interlayer tunneling spectroscopy, which is unique in it's ability to measure properties *inside* HTSC single crystals. This method is specific to strongly anisotropic HTSC, like $Bi_2Sr_2CaCu_2O_{8+\delta}$ (Bi2212), in which mobile charge carriers are localized in double CuO_2 layers, while the transverse (*c* axis) transport is due to interlayer tunneling.[9,10] Interlayer tunneling has become a powerful tool for studying both electron[3,7,11] and phonon[12] DOS of HTSC. It has several important advantages compared to surface tunneling techniques: (i) it probes bulk properties and is insensitive to surface deterioration or surface states;[13] (ii) the current direction is well defined; (iii) the tunnel barrier is atomically perfect and has no extrinsic scattering centers; (iv) mesa structures are mechanically stable and can sustain high bias in a wide range of temperatures (T) and magnetic fields (H).

Here I present a systematic *O*-doping-dependent interlayer tunneling study of Bi2212. The spectroscopic resolution was improved by decreasing in-plane mesa sizes, thus avoiding stacking faults and self-heating in the mesas.[14] This way it was possible to trace the SG and the PG at $T\sim T_c$ and analyze ''closing'' of the PG at a characteristic temperature T^*. The obtained doping phase diagram exhibits a critical doping point for appearance of the PG and a characteristic crossing of the SG and the PG close to the optimal doping. This points towards coexistence of two different, competing order parameters in HTSC. Experimental data indicate that the SG can either form a combined gap with the PG or remain uncombined at $T<T_c$ and that the interlayer tunneling

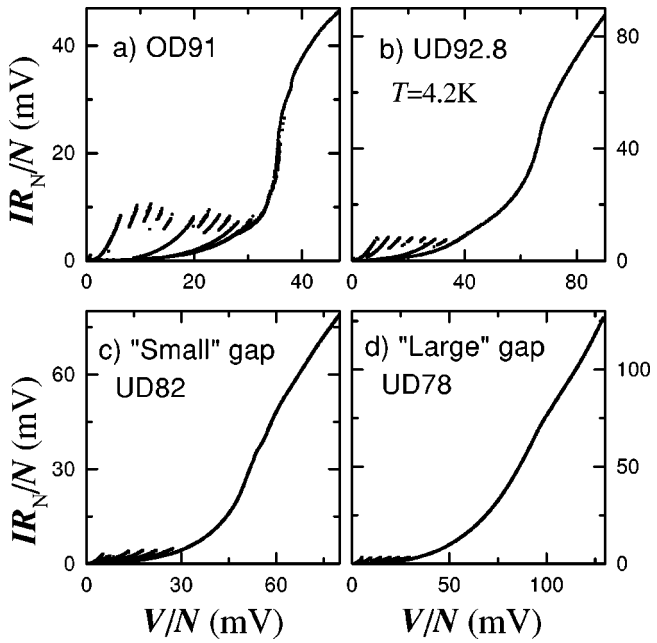

FIG. 1. Normalized IVC's per junction at $T=4.2$ K for Bi2212 mesas with different *O* doping. (a) OD $T_c=91$ K, (b) slightly UD $T_c=92.8$ K, (c) UD $T_c=82$ K the small-gap case; (d) UD $T_c=78$ K the large-gap case.

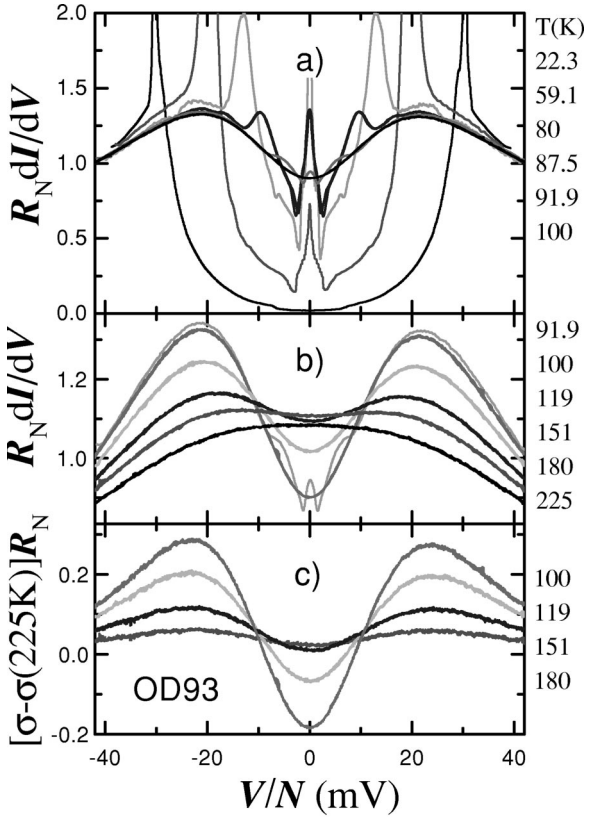

FIG. 2. $dI/dV(V)$ curves for a slightly OD sample $T_c = 93$ K. (a) Below and just above T_c; (b) just below and above T_c; (c) with a subtracted parabolic background.

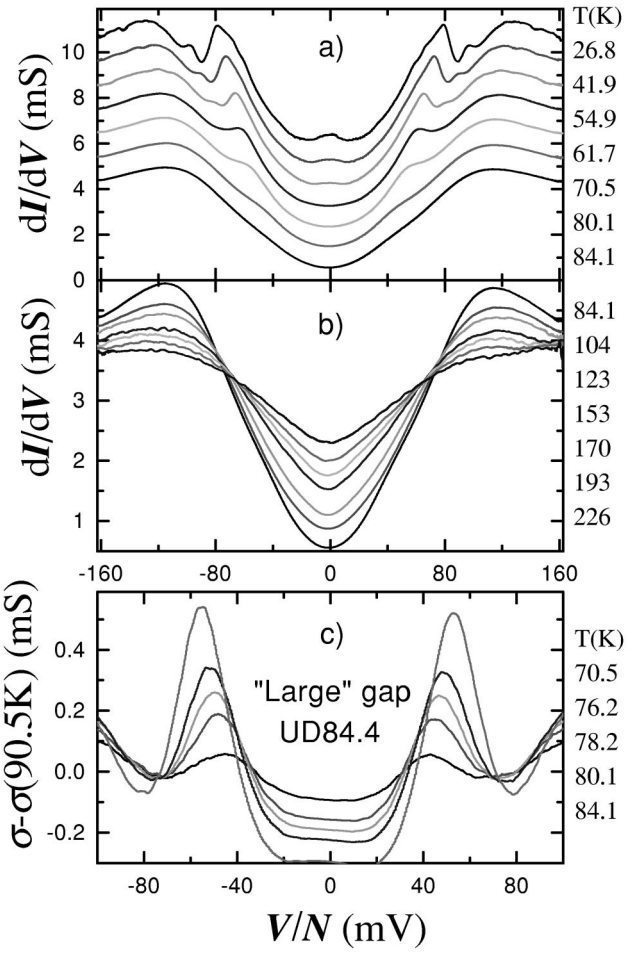

FIG. 3. dI/dV curves for the large-gap case, UD sample $T_c = 84.4$ K. (a) Below T_c (curves are shifted for clarity), (b) above T_c, and (c) curves with a subtracted PG background in the vicinity of T_c. Note different scales in (a), (b), and (c).

is predominantly coherent in OD samples, but becomes progressively incoherent with decreasing doping.

Small mesa structures, with areas $A = 10-30$ μm^2, containing $N = 5-12$ intrinsic junctions, were made on top of Bi2212 single crystals.[3] The fabrication was highly reproducible: all mesas on the same crystal exhibited similar behavior, independent of A and N. UD crystals were prepared by annealing in vacuum at 600 °C.

Figure 1 shows current-voltage characteristics (IVC's) per junction at 4.2 K for different doping. A characteristic knee in IVC's is clearly seen, followed by a normal resistance branch R_N. The knee is strongly suppressed both by T^3 and H,[7] while R_N is almost T,H independent. Such behavior is typical for SIS-type tunnel junctions, in which the knee occurs at a sum-gap voltage $2\Delta_{SG}/e$, where Δ_{SG} is the maximum SG. Multiple branches at low bias correspond to one-by-one switching of junctions from a supercurrent to a quasiparticle (QP) branch. QP branches carry important information: (i) the maximum spacing between QP branches δV_{QP} is an additional parameter for estimation of the SG; (ii) the extent of QP branches along the vertical axis in Fig. 1 represents the $I_c R_N$ product per junction, which is a critical parameters of a Josephson junction.

Figures 2 and 3 show tunneling conductance $\sigma = dI/dV$ curves for slightly OD and UD samples, respectively. Below T_c a sharp peak, corresponding to the knee in IVC's, is seen. The peak voltage, V_{peak}, decreases as $T \to T_c$. Above T_c the peak disappears, but a distinctly different dip-and-hump structure remains, representing the persisting PG.[3] $T-$ dependencies of the peak (large symbols) and the hump (small symbols + lines) voltages for four samples with different doping are shown in Fig. 4.

For OD samples, V_{peak} can be clearly traced up to T_c and $V_{peak} \to 0$ at T_c, see Figs. 2(a) and 4. Note that $V_{peak}(T \ll T_c)$ is substantially larger than the hump voltage $V_{hump}(T_c)$ in the OD mesa. At ~ 150 K, V_{hump} starts to decrease and vanishes at $T^* \sim 200$ K [see Figs. 2(b) and 4]. Interestingly, IVC's are nonlinear even above T^*, see Fig. 2(b) and $\sigma(V)$ has an inverted parabola shape, which might indicate the presence of van Hove singularity close to Fermi level in slightly OD samples.[15] Details of the PG closing at T^* are important for understanding the origin of the PG. At the first glance $V_{hump}(T \to T^*)$ resembles a BCS-like dependence, typical for a phase transition due to an onset of charge or spin-density waves.[16] However, a different perspective opens when the parabolic background at $T > T^*$ is subtracted, see Fig. 2(c). In such a plot the PG simply "fills in" at $T^* \simeq \Delta_{PG}$ without a significant change in V_{hump}. This may indicate that there is a smooth crossover rather than a true phase transition at T^*.

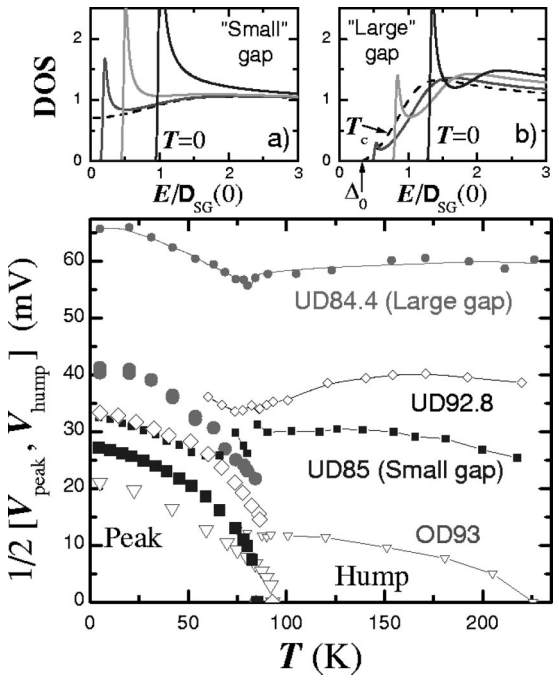

FIG. 4. T dependencies of $\frac{1}{2}V_{peak}$ ($\sim$SG, large symbols) and $\frac{1}{2}V_{hump}$ ($\sim$PG, small symbols + lines) for slightly OD (triangles) and UD (diamonds) samples and for UD samples with small (squares) and large (circles) gaps. Insets (a), (b) show scenarios for formation of small and large gaps at four different temperatures from 0 to T_c (dashed lines).

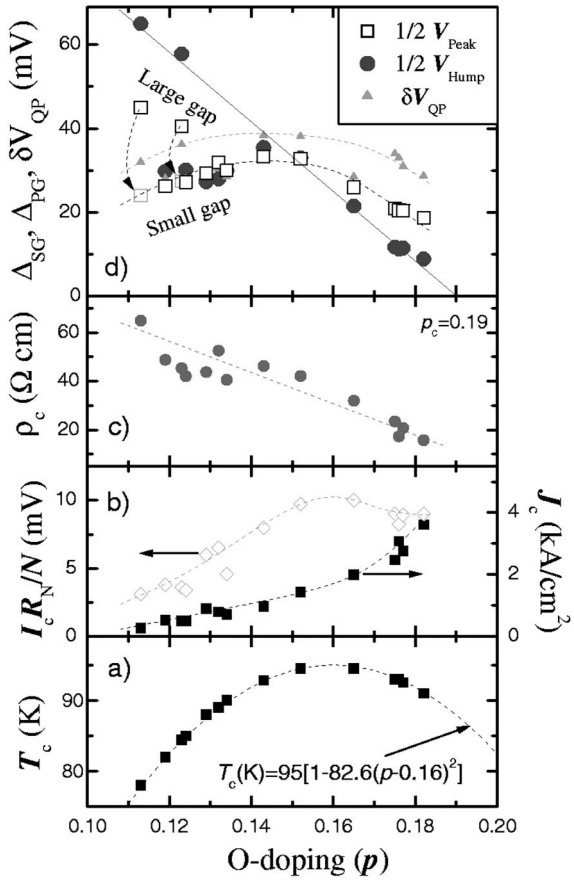

FIG. 5. Doping dependencies of (a) T_c, (b) J_c, and I_cR_N. It is seen that I_cR_N decreases dramatically with doping, due to progressively incoherent nature of the interlayer tunneling. (c) ρ_c at large bias; (d) the doping phase diagram of Bi2212: $\frac{1}{2}V_{peak}$(4.2 K) (open squares), $\frac{1}{2}V_{hump}$(100 K) (solid circles), δV_{QP}(4.2 K) (triangles). A characteristic crossing of the SG and the PG and the existence of critical doping point, $p_c \simeq 0.19$, are clearly seen.

The behavior of the SG in UD samples at $T \rightarrow T_c$ is one of the most important and yet controversial issues.[3,8] For UD samples the peak is much weaker than for OD samples even at low T, cf. Figs. 2(a) and 3(a), and it rapidly smears out with increasing T. The contrast of the peak can be increased by subtracting the background PG dip-and-hump at $T > T_c$, as shown in Fig. 3(c). Thus V_{peak} can be located at $T \sim T_c$.

UD samples showed two distinct types of behavior, which I refer to as ''small'' and ''large'' gap cases, cf. Figs. 1(c) and 1(d). dI/dV curves for the large gap case are shown in Fig. 3. The behavior of large and small gaps is different: (i) for large gaps, the dip-and-hump is strongly enhanced at the expense of the peak. In Fig. 3 the PG dip-and-hump is clearly recognizable even at low T. For the large (UD84.4) and small (UD85) gap samples, in Fig. 4, ratios of hump to dip conductances $\sigma(V_{hump})/\sigma(0)$ at 100 K are $\sim$5.2 and 1.8, while $\sigma(V_{peak})R_N$ at 4.2 K is $\sim$1.6 and 10, respectively. (ii) For small gaps $V_{peak} \rightarrow 0$ at T_c and decreases with UD together with T_c, while for large gaps V_{peak} remains finite at T_c (even though it drops considerably at T_c) see Figs. 3(c) and 4, and both peak and hump voltages increase with underdoping despite the decrease of T_c. (iii) Noticeably, other parameters, such as ρ_c, J_c, and I_cR_N are similar, implying that the tunneling barrier is not affected.

The observed differences can be explained by the scenarios for formation of small and large gaps, shown schematically in insets (a) and (b) of Fig. 4.

The small gap is developed on top of a modest suppression of the DOS at Fermi level, i.e., when there is no true gap at T_c, which might interfere with the opening SG. Therefore, the peak in dI/dV represents the bare (uncombined) SG, which vanishes at T_c, while the dip-and-hump represent a ''normal'' background, which is hindered by the growing SG. Such behavior was observed for OD, optimally doped[3] and UD samples with the small gap, see Figs. 2(a) and 4.

On the other hand, in the large-gap case the SG is developed on top of a true gap Δ_0, see inset (b) in Fig. 4. Indeed, from Fig. 3(b) it is seen that the PG dip-and-hump flatten with increasing T in a state-conserving manner, characteristic for a ''true'' energy gap in DOS, and $\sigma(V)$ curves intersect in one point, indicating approximately constant value of the PG in the measured T range. Below T_c this causes formation of the combined (Δ_0 and Δ_{SG}) large gap. In agreement with this assumption: (i) the large gap does not vanish, but approaches Δ_0 at T_c, see Figs. 3(a) and 4. (ii) The peak completely disappears at T_c but does not transform into the hump because $eV_{hump} > \Delta_0$, see the dashed line in Fig. 4(b). (iii) The volume of the peak (superfluid density) is small because it builds up from an initially suppressed DOS. (iv) The opening of the SG at $T < T_c$ shifts all DOS features, including the

hump, as shown in Fig. 4(b) of Fig. 4. The *correlated* shift of both the peak and the hump with T for UD84.4 sample, as shown in Figs. 3 and 4, is a strong argument in favor of the combined scenario of the large gap. Similarly, *uncorrelated* T-dependent peak and T-independent hump in the OD93 sample, see Figs. 2 and 4, suggests that the small gap represents the uncombined SG. Interestingly, if we take $V_{peak}(4.2\ \mathrm{K}) - V_{peak}(T_c)$ as a measure of the SG part of the combined gap, it will coincide with the small gap for a similar doping, as shown by arrows in Fig. 5(d). A systematic increase of the hump energy with decreasing T, observed by ARPES,[4] would have been consistent with the combined scenario of the large gap if not for the lack of correlated T dependence of the coherence peak.

Figure 5 shows O doping dependencies of: (a) T_c, dashed line represents the empirical expression, used for estimation of p; (b) the critical current density, J_c, and the I_cR_N product per junction; (c) the tunneling resistivity at large bias $\rho_c = R_N A/(Ns)$. The I_cR_N is an important parameter of a Josephson junction. As Bi2212 is likely to be a d-wave superconductor,[17] the I_cR_N depends both on Δ_{SG} and the coherence (in-plane momentum conservation) of c-axis tunneling (another highly debated issue in HTSC[18]). The I_cR_N is maximum $\simeq \Delta_{SG}/e$ for coherent, and zero for completely incoherent tunneling.[19] For OD mesas $I_cR_N \sim 10$ mV is a considerable fraction ~ 0.6 of Δ_{SG}/e, indicating predominantly coherent nature of the interlayer tunneling. With underdoping, the I_cR_N decreases dramatically at a much faster rate than Δ_{SG}. This indicates that the interlayer tunneling becomes progressively incoherent in UD Bi2212.

Figure 5(d) shows the obtained doping phase diagram of Bi2212. Here I plot $\frac{1}{2}V_{peak}(4.2\ \mathrm{K}) \sim \Delta_{SG}/e$, $\frac{1}{2}V_{hump}(100\ \mathrm{K} > T_c) \sim \Delta_{PG}/e$, and $\delta V_{QP}(4.2\ \mathrm{K})$. It is seen that the small gap ($\sim$ SG) shows a similar tendency as T_c and decreases both on OD and UD sides. This is also supported by a correlated behavior of δV_{QP}. In contrast, the large gap ($\sim$PG) increases approximately linearly with underdoping, as shown by the solid line. The PG and the SG lines cross at about the optimal doping, $p = 0.16$. On the OD side the PG becomes considerably less than the SG and shows a clear tendency to vanish at the critical doping point, $p_c \simeq 0.19$. This speaks in favor of a nonsuperconducting origin of the PG,[6] consistent with earlier observations of different T^3 and H^7 dependencies of the SG and the PG. Within such a scenario, a suppression of superconductivity (decrease of T_c, Δ_{SG}, the superfluid density, etc.) in UD HTSC is caused by appearance of the competing order parameter (PG), e.g., due to strengthening of antiferromagnetic correlations and formation of spin-density waves. Note that a similar phase diagram, attributed to competition between superconducting and antiferromagnetic orders, was reported for heavy fermion superconductors.[20]

At present, the reason for appearance of either small or large gaps in UD samples is unclear. However, it is not due to irreproducibility of fabrication (all mesas on the same crystal show the same behavior) or macroscopic defects (regular QP branches are observed in both cases). Presumably, the ambiguity is connected with a microscopic inhomoginiety of UD crystals.[21] The presence of ambiguity obscures identification of the genuine HTSC behavior in the UD region. However, there is no ambiguity for overdoped and optimally doped samples. Therefore, conclusions that there is a critical doping point in HTSC phase diagram and that the SG and the PG cross rather than merge near the optimal doping are robust.

In summary, O doping dependence of Bi2212 was studied using high-resolution interlayer tunneling spectroscopy. We were able to simultaneously trace the superconducting gap and the c-axis pseudogap at $T \sim T_c$ and analyze ''closing'' of the PG at T^*. The obtained doping phase diagram exhibits a critical doping point for appearance of the PG and a characteristic crossing of the SG and the PG close to the optimal doping, indicating a competing nature of two coexisting order parameters in HTSC. In UD samples, the SG can either form a combined gap with the PG or remain uncombined at $T < T_c$, but the bare SG vanishes at $T \simeq T_c$ for all studied doping levels. Analysis of I_cR_N vs Δ_{SG} indicates that the interlayer tunneling is predominantly coherent in OD, but becomes progressively incoherent in UD samples.

[1] I. Giaevier, Phys. Rev. Lett. **5**, 464 (1960).
[2] G. Deutscher, Nature (London) **397**, 410 (1999).
[3] V.M. Krasnov *et al.*, Phys. Rev. Lett. **84**, 5860 (2000).
[4] J.C. Campuzano *et al.*, Phys. Rev. Lett. **83**, 3709 (1999).
[5] A.V. Puchkov, D.N. Basov, and T. Timusk, J. Phys.: Condens. Matter **8**, 10 049 (1996).
[6] J.L. Tallon and J.W. Loram, Physica C **349**, 53 (2001).
[7] V.M. Krasnov *et al.*, Phys. Rev. Lett. **86**, 2657 (2001).
[8] M. Kugler *et al.*, Phys. Rev. Lett. **86**, 4911 (2001).
[9] R. Kleiner *et al.*, Phys. Rev. Lett. **68**, 2394 (1992).
[10] V.M. Krasnov *et al.*, Phys. Rev. B **59**, 8463 (1999).
[11] M. Suzuki and T. Watanabe, Phys. Rev. Lett. **85**, 4787 (2000).
[12] K. Schlenga *et al.*, Phys. Rev. B **57**, 14 518 (1998).
[13] A. Lanzara *et al.*, Nature (London) **412**, 510 (2001).
[14] V.M. Krasnov *et al.*, J. Appl. Phys. **89**, 5578 (2001); V.M. Krasnov, cond-mat/0109079 (unpublished).
[15] O.K. Andersen *et al.*, Phys. Rev. B **49**, 4145 (1994).
[16] R.S. Markiewicz, C. Kusko, and V. Kidambi, Phys. Rev. B **60**, 627 (1999); F. Onufrieva and P. Pfeuty, *ibid.* **61**, 799 (2000); S. Chakravarty *et al.*, *ibid.* **63**, 094503 (2001).
[17] C.C. Tsuei and J.R. Kirtley, Rev. Mod. Phys. **72**, 969 (2000).
[18] P.W. Anderson, Science **279**, 1196 (1998).
[19] Y. Tanaka and S. Kashiwaya, Phys. Rev. B **56**, 892 (1997).
[20] N.D. Mathur *et al.*, Nature (London) **394**, 39 (1998).
[21] T. Cren *et al.*, Phys. Rev. Lett. **84**, 147 (2000).